

BEAM POSITION MONITORING AND FEEDBACK STEERING SYSTEM  
AT THE PHOTON FACTORY

T. Katsura, Y. Kamiya, K. Haga, T. Mitsuhashi  
Photon Factory, National Laboratory For High Energy Physics  
Tsukuba, Ibaraki 305, Japan

R.O. Hettel  
Stanford Synchrotron Radiation Laboratory  
SLAC Bin 69, Stanford, Calif. 94305, U.S.A.

ABSTRACT

A version of the beam steering servo system developed at SSRL was used to vertically position and stabilize the synchrotron radiation beam on Beam Line 21 at the Photon Factory. System components included a photon beam position monitor located 12 meters from the bend magnet source point, a servo controller containing frequency compensation and gain circuits, and a 3-magnet orbital bump steering system. Two types of position monitor, one an ion chamber and the other an in-vacuum device, were used in the system. Vertical beam position noise spectra obtained from these monitors showed predominant peaks occurring at 14.5 Hz, 50 Hz, and at several other frequencies in the 1 to 100 Hz range, having typical RMS amplitudes in the 1 to 5 micron range. The closed-loop system was able to reduce low frequency positional offsets ( $< 0.1$  Hz) by a factor of 1000, and the 14.5 Hz oscillation by a factor of 6.

INTRODUCTION

The small vertical size of the synchrotron radiation beams originating from a multi-GeV storage ring, typically a few millimeters or less at experimental stations, in most cases makes the vertical positional stability of these beams critical to the quality of collected data. Whereas most of the users at the Photon Factory seem content with the present level of beam stability at the laboratory, there are a few (mostly users of focused beam lines) that report a degradation in signal-to-noise ratio or a loss of data resolution caused by long and short term vertical beam motion on the submillimeter level. Other synchrotron radiation laboratories also report observing various degrees of beam position instability; noise spectra reveal principal components occurring at frequencies typically less than 100 Hz<sup>1,2</sup>.

The positional stability of the primary photon beam within a beam channel, before any optical elements are encountered, is strictly a function of the stored beam orbital stability at the beam line source region. In particular, small orbital angle changes at the source region are multiplied by the many meters distance to the experiment to produce amplified position changes there. Stabilizing the position of the primary photon beam is thus a matter of stabilizing the charged beam orbit.

The position of the photon beam itself near the experimental station should be monitored to give a sensitive indication of stability. With such a monitor, and a localized orbit correction system that does not affect other beam line source points, a closed-loop beam stabilization system can be devised.

It was decided by members of the Light Source group at the Photon Factory to implement a prototype steering servo system on their diagnostic Beam Line (BL) 21, similar to the type developed at SSRL.<sup>4</sup> This beam line was subsequently extended beyond the shielding wall to provide a position monitoring site several meters from its bend magnet source point<sup>5</sup>.

An in-vacuum photoemission detector, consisting

of two tungsten wires stretched horizontally across the beam path at 10 meters from the source and separated vertically, was installed. In addition, a split-anode ion chamber monitor of the type used at SSRL was placed inside the experimental hutch, located 12 meters from the source, where X-rays have been extracted from the evacuated beam channel through an aluminum window. Both of these devices yield a vertical position error signal proportional to the difference between the upper and lower sensor currents, have a positional resolution in the micron range, and have a bandwidth typically to a few kilohertz or less by the current-detecting electrometer amplifiers. With these monitoring systems, a successful vertical position stabilizing system was configured.

EXPERIMENTAL APPARATUS

Three main components are needed to configure a basic beam steering servo system: a beam position monitor, an orbit correction system, and a servo controller that enables the first two elements to be integrated into a stable closed-loop system (Fig. 1).

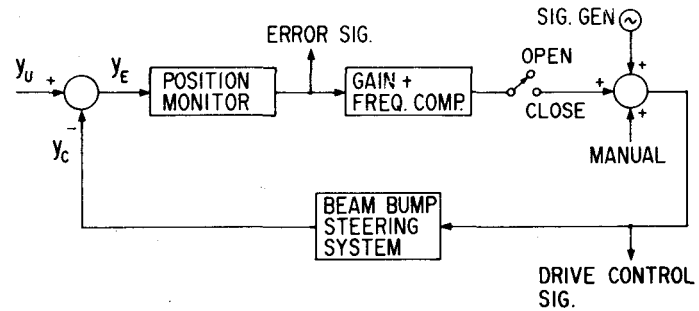


Fig. 1. Beam steering servo system.  $Y_U$ ,  $Y_C$ , and  $Y_E$  represent the uncorrected beam position, the corrective position shift, and the resulting position error, respectively.

The components may be physically located in widely separated areas of the storage ring facility. At the Photon Factory, the position monitor was situated in the beam line near the experimenter station, while the corrector magnets were inside the ring and the magnet power supplies were in the basement beneath the ring. The servo controller is usually located in the ring control room, although it was located near the experimenter station for the tests described here.

Beam Position Monitor

Two types of monitors were used to detect vertical photon beam position and positional noise in BL-21. One was a split-anode ion chamber shown schematically in Figure 2, situated ~12 meters from the beam line source point. The two triangular anode plates collect ions produced by the X-ray beam passing between anode and cathode plates (the cathode was held at -300 volts) in a chamber filled with

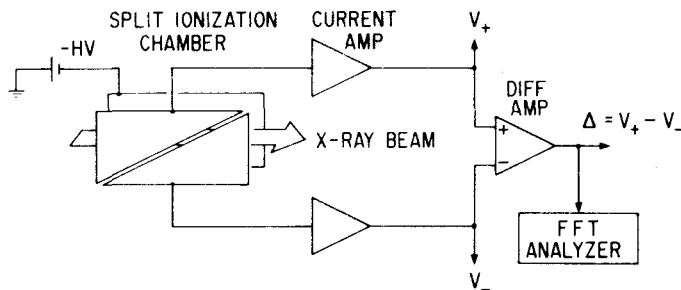


Fig. 2. Ion chamber position monitor. The difference between upper and lower ionization currents is proportional to beam displacement from the chamber center.

argon at slightly more than atmospheric pressure. The triangular plates have base and height sizes of 8 cm and 3 cm respectively, surrounded by a guard ring, and the anode and cathode plates are separated by 6 mm. Incoming beam is masked so that synchrotron light does not strike the plates directly. Upper and lower anode currents are detected with Keithley 427 current amplifiers which maintain the anode potential at virtual ground. The vertical displacement of the beam from the monitor's electrical center is proportional to the difference  $\Delta$  between the upper and lower currents divided by their sum  $\Sigma$ .

The second position monitor used in the system consists of two photoelectron-emitting tungsten wires stretched horizontally across the beam path within the evacuated beam channel at a distance of  $\sim 10$  meters from the beam source. The wires are separated vertically by 3 cm and sense the upper and lower low photon energy tails of the X-ray beam as it passes between them. The wires are held at ground potential by Keithley current amplifiers; cleaning electrodes are provided to collect the photoelectrons. The monitor is not intended to give an accurate value for beam displacement from the centerline; rather, it gives an accurate indication of beam centering ( $\Delta = 0$ ) and is perfectly suitable for use in a servo system that maintains this centering.

Each monitor is mounted on a remotely controlled vertical translation stage so that its electrical center can be aligned with the nominal centerline of the photon beam. The bandwidth of each monitor's error signal is limited by that of the current amplifiers. The bandwidth typically used for this application is  $\sim 3$  kHz (Keithley 427 risetime setting = 0.1 msec), more than an order of magnitude greater than that for the orbit correction system. Beam position noise spectra were obtained from the monitors' error signals using an FFT spectrum analyzer (Advantest 9404).

#### Orbit Correction System

Orbit corrections localized to a small region of the storage ring surrounding the source point can be generated using a system of three corrector magnets driven in parallel with appropriately scaled currents derived from a common control signal (Fig. 3). For BL-21, only two of the three vertical correctors (VD30, VD32 and VD34) are needed to generate the localized beam bump: the middle magnet (VD32) is obviated because of the 180 degree betatron phase separation between the two end magnets.

Each corrector magnet is energized by a current-actuating power supply (Kikusui PAD55-3LS). The control signal for each supply is formed by summing the signal produced by the steering servo system with a signal generated by the computer orbit control

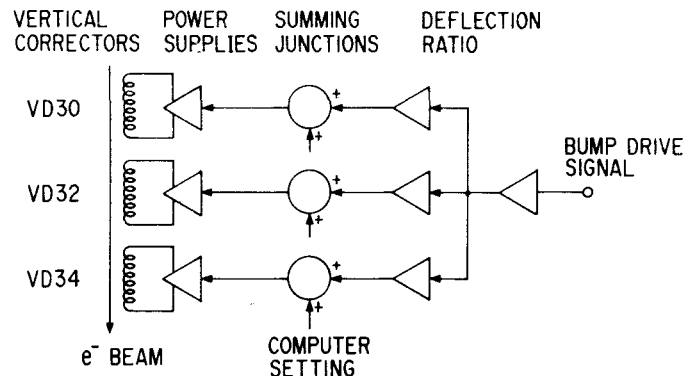


Fig. 3. Orbital bump system for steering BL-21.

program, so that beam line steering corrections are superposed on nominal orbit configuration.

The vertical change in orbit at the BL-21 source point caused by an angular kick  $\delta$  in the first bump magnet is translated into a vertical position deflection  $\Delta y$  of the photon beam. At L meters from the source point,  $\Delta y = (Y + LY')\delta$ , where  $Y = 6$  mm/mrad,  $Y' = 2$  mrad/mrad, and  $\delta$  is specified in milliradians.  $Y$  and  $Y'$  are constants of the ring lattice and characterize the positional and angular effects of the bump at the source point. At the 12 m position monitor location, the bump produces 30 mm per mrad of corrector deflection.

#### Steering Servo Controller

The function of the steering servo controller, besides providing a means to adjust beam position and open and close the feedback loop, is to process the position monitor error signal so that a stable closed system capable of reducing position offset at the monitor can be configured. The processing is accomplished with a system of frequency compensation and gain circuits whose properties are determined primarily from the response characteristics of the orbit correction system.

#### EXPERIMENTAL PROCEDURES AND RESULTS

##### Position Monitor Alignment, Calibration, and Noise Measurements

The photon beam was swept vertically in the beam line to determine the range of unoccluded beam movement, defined by the vacuum duct and of upstream slit apertures, within each position monitor. The monitors were then shifted vertically so that their electrical centers approximately coincided with the respective aperture midpoints. The steering bump strength parameter, defined in terms of millimeters of position change at the monitor per ampere of bump magnet current, was determined by steering the beam vertically and measuring with a micrometer dial gauge the vertical translation of the monitor needed to recenter the beam within it. The bump strength parameter was found to be 9.1 mm/amp for the ion chamber monitor, and 8.1 mm/amp for the upstream in-vacuum wire monitor. Signal currents were on the order of 70 nA for the ion chamber monitor, and 10 nA for the in-vacuum monitor, with  $\sim 20$  mA of stored 2.5 GeV beam.

With the monitors aligned to the optimum beam centerline, their responses to beam position offsets were measured. The ion chamber response was highly linear over an 11 mm range, being limited mainly by upstream vertical slits. The normalized data points

$\Delta / \Sigma$  were highly insensitive to a factor of two change in stored beam current. The wire monitor response displayed an unexpected degree of linearity over a 4 mm range.

Position noise spectra were measured using the FFT spectrum analyzer. The spectra obtained from the two monitors agreed very closely in frequency content, and varied slightly in relative amplitudes. Most of the noise components are concentrated in the DC to 100 Hz range (Fig. 4); higher frequency components occur principally at harmonics of 50 Hz, the line power frequency, and have very low energy.

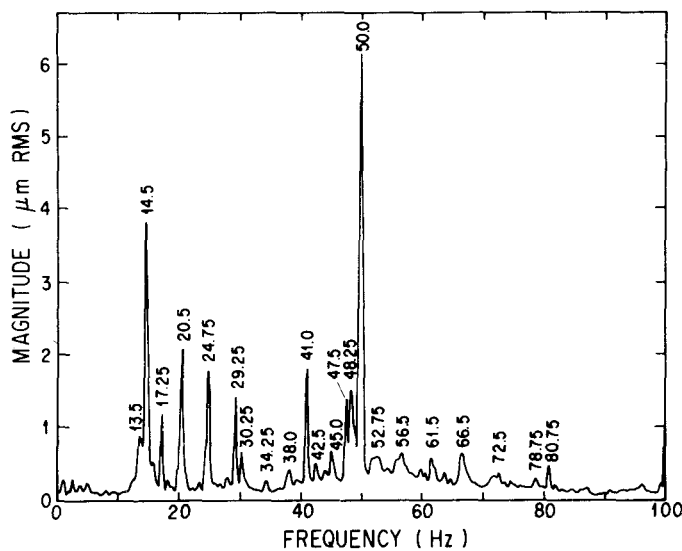


Fig. 4. Vertical beam position noise spectrum taken with the wire monitor. Frequency components agree closely with the ion chamber spectrum, shown in the upper frame of Fig. 7.

#### Frequency Response of the Orbit Bump System

The frequency response of the current power supplies driving their corrector magnet loads was determined by driving the input of one supply with a variable frequency control signal and monitoring the

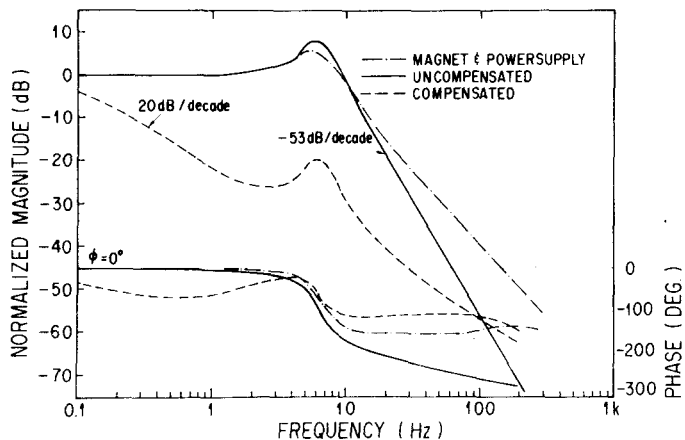


Fig. 5. Steering system response using the corrector magnet primary windings (2100 turns). Responses of the magnet/power supply system and the total steering bump system, before and after frequency compensation, are shown.

output current with a 0.1 ohm resistive shunt. The FFT Analyzer had two channel inputs and could be used to measure the response magnitudes and phases plotted in Figure 5. A 6 dB resonant peak in the response curve near 5.5 Hz was observed. Measurements beyond ~200 Hz were unreliable because of the very small output current levels.

The response of the complete beam bump/position monitor system was ascertained by driving the beam with a variable frequency bump control signal and measuring the response of the position monitor. The resulting curves for this uncompensated steering system are also shown in Figure 5. Since the position monitor bandwidth was set to ~3 kHz, these curves essentially represent the response of the power supply and magnet system driving the beam. The difference between these and the previous set of curves is due primarily to the magnetic field response of the corrector magnets themselves, and to the frequency-dependent attenuation of the fields penetrating the vacuum chamber caused by eddy currents induced in the conducting chamber walls. Again a resonant response peak was observed, this time near 6 Hz.

#### Feedback Loop Compensation and Performance

To guarantee a stable closed-loop configuration, the open-loop servo system response must conform to well-known stability criteria. In simplified terms, this meant that the uncompensated orbit bump system response had to be modified with the addition of frequency compensation and gain circuits so that the response magnitude curve descended at higher frequencies at an approximate rate of 20 dB per frequency decade and crossed the 0 dB line at a frequency where the response phase lag was less than 180 degrees by a sufficient margin (~45 degrees). A simple compensation network was devised that yielded the compensated open-loop response (normalized to 0 dB at DC) shown in Figure 5. Before trying closed-loop operation, it was not known exactly what effect the still-present resonant peak would have.

In closed-loop mode, the system bandwidth was increased from at first a very low value (< 0.1 Hz) to a maximal value near 7 Hz by increasing the servo gain. As the bandwidth neared 7 Hz, a resonant amplification of the beam position noise components in this frequency range was observed. It was discovered that magnet/power supply system response was dependent on control signal amplitude for frequencies contained in the resonant peak. In particular, increased input amplitude at 7 Hz was seen to add ~20 degrees of phase lag at that frequency, thereby reducing the servo phase margin to a point where the system approached instability. The system operated stably with no increase in noise amplitudes when the bandwidth was restricted to ~1 Hz. A factor of ten reduction DC position offset was obtained at this bandwidth. It appeared that the only way to increase the system bandwidth and achieve greater noise suppression was to eliminate the bump resonance.

#### Wideband Response Using Secondary Corrector Windings

The resonant peak in the magnet/power supply response was determined to be caused by the parallel connection of the highly inductive corrector coils (2100 turns/pole on a solid iron core, with a total inductance of ~1 henry and a DC resistance of 10 ohms) and a large filter capacitor at the output of the power supply. Lower inductance correctors were fashioned by winding secondary coils of 120 turns on top of the original coils. Although the large filter capacitor was needed for power supply stability while driving the original corrector load, it was found to

be unnecessary for driving the new lower resistance, lower inductance load and was removed. The resulting supply resonance-free output current and uncompensated steering bump frequency response curves using these new correctors are shown in Figure 6. An order of

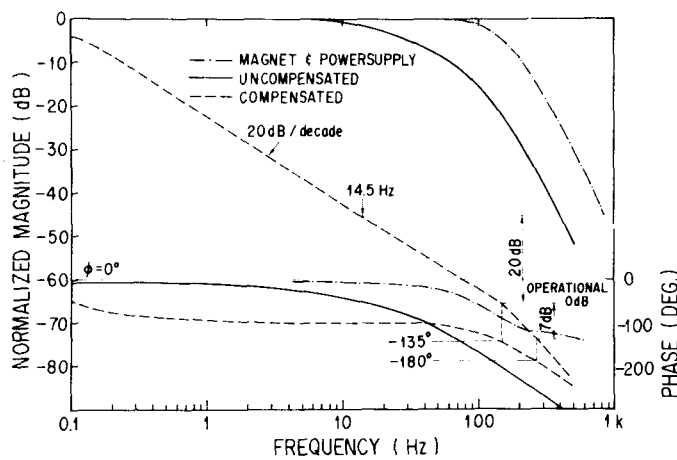


Fig. 6. Steering system response using the corrector secondary windings (120 turns).

magnitude increase in bandwidth was gained at the expense of a similar magnitude loss in corrector strength. No significant feedthrough of alternating current from secondary to primary windings (transformer action) was seen.

The steering servo system now consisted of one set of strong, low frequency correctors under the computer control for affecting large orbit and beam steering changes, together with a set of higher frequency correctors used for making small corrections and for the closed servo loop. The compensated open-loop system response (Fig. 6) promised up to a factor of 10 reduction of the prominent 14.5 Hz positional noise peak when operating at a maximal gain

in closed-loop mode. The maximum attenuation actually achieved at this frequency after closing the servo loop was measured to be a factor of 6 (Fig. 7). The predicted attenuation may have been achievable if the power supply control signal amplitudes needed to generate small higher frequency corrections (> 500 Hz) with the relatively weak correctors had not reached maximum allowable (unclipped) levels, thereby causing a degree of control circuit saturation, before the predicted servo gain was reached. Still, this configuration attenuated frequencies of  $\sim 1$  Hz and 0.1 Hz by factors of 100 and 1000 respectively.

#### CONCLUSIONS AND FURTHER DEVELOPMENT

The vertical position noise spectrum for the synchrotron light beam shows peaks mostly below 50 Hz, having RMS amplitudes of a few microns at the 12 m monitor location. Observed peak amplitudes may be a factor of 5 or so greater, and of course the instantaneous displacement of the beam at any time depends on the superposition of all frequency components together with their relative phases. A long term positional drift of  $\sim 0.1$  mm/hr was also seen.

A search for beam noise sources is underway, for example, an array of vibrometers has been set up to measure the mechanical vibration modes of the storage ring and building. The influence that various potential mechanical noise sources, such as the liquid helium refrigerator, air conditioners, vacuum pumping system, etc., have on stimulating these modes can be determined by turning these devices off one by one. The results of this search will soon be published elsewhere<sup>4</sup>.

Although the steering servo system bandwidth and performance was effectively improved by two orders of magnitude by using the secondary corrector windings, still higher bandwidth and attenuation levels can be reached by changing the corrector design. It is expected that a factor by two or more improvement can be gained by doubling the number of secondary windings on the existing cores, while certainly much greater bandwidths can be reached if high frequency cores used.

The level of steering feedthrough to the rest of the ring, best measured with the highly sensitive photon monitors located meters from the ring, will be investigated in the near future when such monitors are installed in BL-10 and BL-12. In the meantime, the degree of isolation obtained by a bump similar to that for BL-21, configured at an equivalent location elsewhere in the ring, will be measured using the photon monitor on BL-21.

#### ACKNOWLEDGMENT

We are indebted to both K. Huke, director of the Photon Factory Light Source, and H. Winick, deputy director of SSRL, for their arrangement and support of this collaboration. We are also grateful to members of the Photon Factory Ring group for their operational contributions and unceasing cooperation.

#### REFERENCES

1. R.O. Hettel, IEEE Trans. on Nucl. Sci., Vol. NS-30, 2228 (1983)
2. L.H. Yu et al., IEEE Trans. on Nucl. Sci., Vol. NS-32, 3394 (1985)
3. Photon Factory Activity Report, 1984/85, pg. 62.
4. K. Huke et al., to be submitted to Jpn. J. of Appl. Phys.

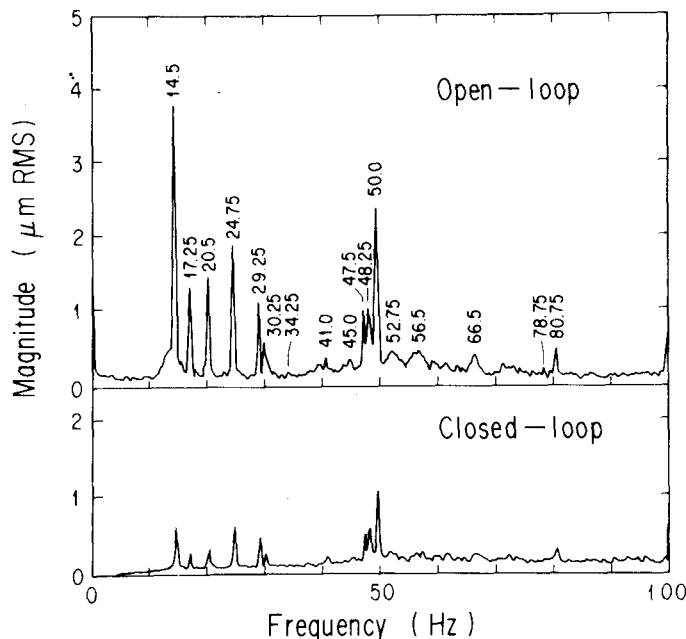


Fig. 7. Position noise spectra taken before and after closing the steering servo loop. The 14.5 Hz peak is suppressed by a factor of 6.